MOEM

Modern Electronic Materials 2020; 6(4): 125–132
DOI 10.3897/j.moem.6.4.65351

Research Article

Technology of thermally stimulated diagnostics of anisotropy and optical axes in crystals

Viktor M. Timokhin[1,2], Vladimir M. Garmash[3], Valentin A. Tedzhetov[2]

1 Admiral Ushakov State Maritime University, 93 Lenin's Avenue, Novorossisk, Krasnodar Region 353900, Russia

2 National University of Science and Technology MISiS, 4 Leninsky Prospekt, Moscow 119049, Russia

3 "Scientific and Technological Center of Unique Instrumentation" of the Russian Academy of Sciences, 15 Butlerova Str., Moscow 117342, Russia

Corresponding author: Viktor M. Timokhin (t.v.m@inbox.ru)

Received 11 March 2020 ♦ **Accepted** 26 September 2020 ♦ **Published** 30 December 2020

Citation: Timokhin VM, Garmash VM, Tedzhetov VA (2020) Technology of thermally stimulated diagnostics of anisotropy and optical axes in crystals. Modern Electronic Materials 6(4): 125–132. https://doi.org/10.3897/j.moem.6.4.65351

Abstract

For implementing the technology of thermally stimulated diagnostics of anisotropy and optical axes in crystals, the sample is thermostated at a temperature not exceeding the melting point, an electric field not exceeding the breakdown field is applied to the sample and polarization is produced for a time greater than the relaxation time at this temperature. After that, without switching off the electric field, the sample is cooled to the liquid nitrogen temperature, following which the field is switched off, the sample is linearly heated to a temperature above the polarization temperature and the resultant thermally stimulated depolarization (TSD) spectra taken along and perpendicular to the optical axis of the crystal are examined. When comparing the spectra the presence of anisotropy is detected and the direction of the optical axes is determined from the magnitude and presence of the TSD maxima.

Keywords

diagnostics, crystalline materials, anisotropy, optical axis, thermally stimulated currents.

1. Introduction

Optically uniaxial α-$LiIO_3$ single crystals possess unique optical, electrical, pyroelectric and piezoelectric properties and are used as short wave frequency doublers in various semiconductor lasers for laser-beam ship guidance applications. There are several methods of optical axis diagnostics [1–3] which are described hereinbelow. However they are either complex or not suitable for detecting the presence of anisotropy since they are used for determining the direction of the optical axis in crystals which are known to be anisotropic.

The method of determining the direction of the optical axis for a phase-anisotropic crystalline λ/4 wafer was described earlier [1]. This method is implemented with the aid of an optical system containing polarizers installed perpendicular to its axis, the tested phase-anisotropic crystalline λ/4 wafer, a phase compensator, and an analyzer crossed with the polarizer. Rotation of the test crystalline wafer around the optical system axis produces a conoscopic figure in the form of a bright Maltese cross. The position of the optical axis in the entrance face plane of the tested phase-anisotropic crystalline λ/4 wafer is determined based on its parallelism with the line connecting two black points in the conoscopic figure. However this method is not suitable for detecting anisotropy because the test crystal is *a priori* anisotropic. Also known is the method of determining the type, number, activation energy, relaxation time and activation volume of crystal lattice defects

in dielectrics and semiconductors [2] which includes TSD spectrum measurement for relaxed and compressed materials. However this method is not either applicable for the diagnostics of anisotropy because compressed crystals undergo deformation and their structure and thickness change thus distorting the measurement results.

The closest counterpart of the technology suggested herein by the technical principle and the achieved result is the method of determining the onset temperature of the tunneling effect in dielectrics and electrically insulating materials [3] for which the TSD spectrum of the test crystal is taken, the activation energy is determined, and the presence of the tunneling effect is judged about from the presence of No. 1 low-temperature maximum. Then the dielectric loss tangent spectrum tgδ (*f*, *T*) is measured, the onset temperature of the tunneling effect in the sample being determined as the temperature at which the maxima of the tgδ (*f*, *T*) spectrum no longer shift towards low frequencies due to variations of the sample temperature. However this method is not either intended for the diagnostics of anisotropy in crystals because this does not require measuring the tgδ (*f*, *T*) spectrum but only examining No. 1 maximum of the TSD spectrum.

The aim of this work is to provide a technology of thermally stimulated diagnostics of anisotropy and optical axes in crystals on the basis of TSD spectrum examination. The main objectives of this study are: 1) obtaining TSD spectra in different directions in the 77–473 K temperature range; 2) obtaining thermally stimulated luminescence **(TSL)** spectra and comparing them with the TSD spectra; 3) obtaining electrical conductivity spectra and comparing them with the TSD spectra. The importance of this study is dictated by the necessity of providing a technology of the diagnostics of anisotropy and optical axes in crystalline laser materials used on board marine ships and at onshore facilities, especially those operating at low temperatures.

2. Theory of thermally stimulated depolarization currents

The principle of the thermally stimulated depolarization method **(TSD)** is the non-isothermal electrical relaxation of charged particles due to the fact that when the sample temperature varies following a certain law the material changes from nonequilibrium to equilibrium state. The process is accompanied by energy release which can be detected by measuring the conductivity, thermally stimulated depolarization currents, thermally stimulated luminescence etc. The current *vs* temperature dependences allow one to determine the energy parameters of the electrophysical processes in the sample. The first prototypes of the method were developed in the late 1960s by C. Bicci, R. Fieschi et al. [4, 5].

Theoretical models of thermally stimulated depolarization currents **(TSDC)** were developed earlier [6] but practical TSD methods only found application in the 1980s for studies of ice [7]. The TSD method provides much more information than the dielectric loss method (tg δ and ε*) and provides for higher resolution and accuracy of measurements (by at least two orders of magnitude) [8].

The measurement of thermally stimulated depolarization currents is carried out as follows. The prepared sample is placed between the electrodes, isothermally aged at the polarization temperature T_p, the electric field E_p is applied to the sample and polarization is carried out for the time t_p; this produces an inhomogeneous distribution of carries and an anisotropic orientation of polar molecules in the sample. The electric field also causes migration of free carriers. The pinning of charges shifted through a macro-distance may occur in the vicinity of the electrodes (near-electrode polarization) or inside the crystal. The polarized object is rapidly cooled without switching off the electric field E_p to the temperature T_0 (in the case considered, the liquid nitrogen temperature, i.e., 77 K), and as a result the polarized state is retained for a long time and the relaxation time increases substantially. Then the electric field is switched off, the sample is connected to a V7-30 measuring instrument and heated at a constant rate. As a result a depolarization current is produced in the outer circuit and the maximum corresponding to the specific type of defects appears in the TSD spectrum.

3. Methods of calculating defect parameters by thermally stimulated depolarization current spectra

3.1. Determination of the charge concentration

For determining the total depolarization charge one integrates the area under the $I = f(T)$ curve [8] which is proportional to the concentration of this type of charge (Fig. 1 *a*). The concentration of charged defects corresponding to this TSD maximum is determined as follows:

$$n = \int_{T_0}^{\infty} \frac{j(T)}{\beta d} \mathrm{d}T \qquad (1)$$

where $\beta = \mathrm{d}T/\mathrm{d}t$ is the sample heating rate, d is the sample thickness and j is the current density.

3.2. Determination of the activation energy

3.2.1. Garlick-Gibson method (initial rise method) [8].

The initial rise method is based on the fact that at low temperatures (about the liquid nitrogen temperature) the initial sections of TSD current curves have the following pattern regardless of the relaxation process kinetics:

$$I(T) = I_0 \exp\left(\frac{U_a}{kT}\right). \qquad (2)$$

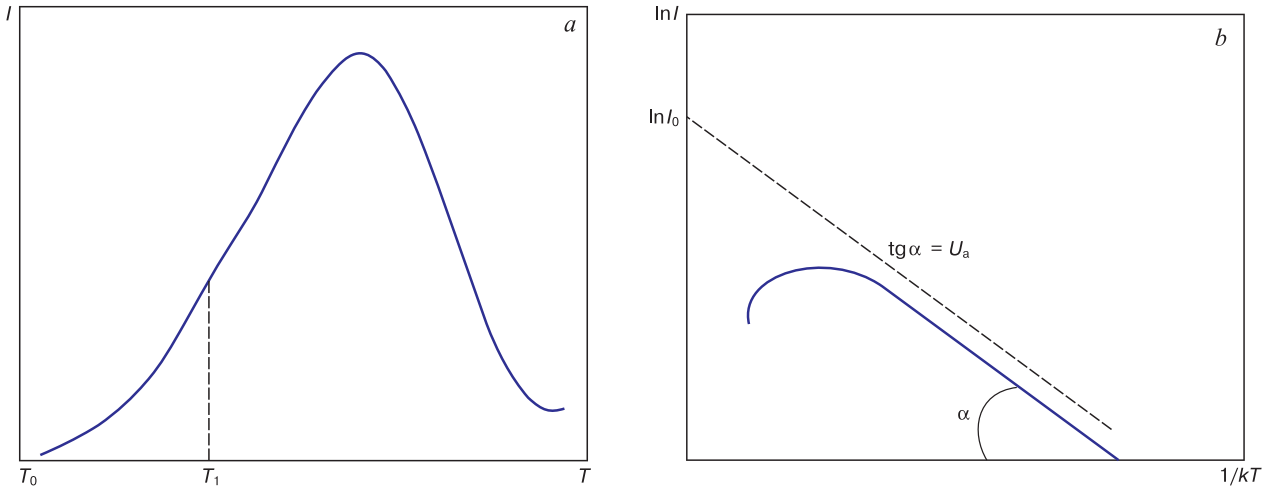

Figure 1. Defect parameter determination from TSD spectra with the Garlick–Gibson method: (*a*) TSD temperature dependence in linear heating mode, (*b*) TSD curve in Arrhenius coordinates with initial rise section.

It can be seen from Eq. (2) that the initial section of the TSD current curve in the Arrhenius coordinates ($\ln I \sim 1/kT$) is a straight line (see Fig. 1*b*) and therefore one can graphically determine the activation energy U_a of the electrically active defects with a 5% accuracy.

3.2.2. Partial thermal cleaning method

This method was first suggested in an earlier work [6]. In our test crystals the number of relaxer types is 5–6. Thus some maxima in the TSD spectrum are superimposed. One should therefore separate each maximum in order to obtain the initial rise and drop, i.e., suppress the low-temperature TSD maximum preceding the studied one. To this end the polarized sample is heated from $T_0 = 77$ K to the temperature that is 10 K higher than the temperature T_m of the maximum to be suppressed (Fig. 1, Curves *1* and *2*). Then the sample is rapidly cooled to a temperature at which the current drops almost to zero in accordance with Fig. 2 (Curves *2* and *3*). Then the sample is linearly heated at the same rate. As a result the low-temperature maximum disappears, i.e., the relaxers that produce this maximum are misoriented, and the initial rise of the next maximum is achieved (e.g., the next maximum with the initial rise is separated, see Curves *3*, *4* and *1*) from which one can calculate the parameters of the defect that produces this maximum using the Garlick–Gibson initial rise method. After that, the operation is repeated for the next maximum.

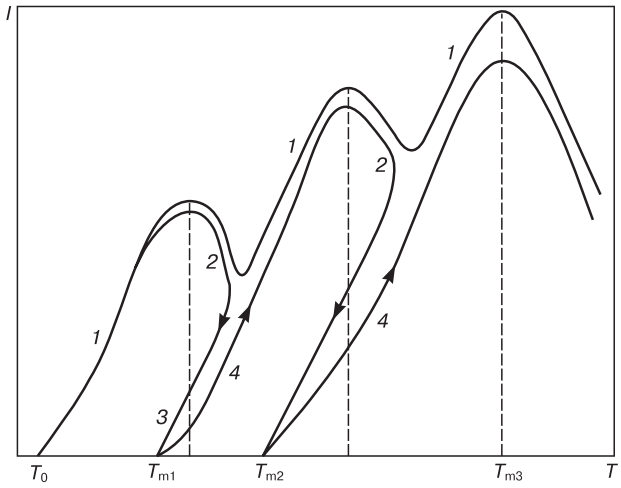

Figure 2. Partial thermal cleaning method for TSD currents: (*1*) linear heating, (*2*), (*3*) and (*4*) partial thermal cleaning mode.

4. Experimental

In this work we used the methods of thermally stimulated depolarization currents, electrical conductivity and thermally stimulated luminescence **(TSL)**. The instruments were a V7-30 electronic voltmeter-electrometer, a V6-21 voltmeter, stabilized power sources, VM-538 and VM-507 impedance meters, Dewar flasks with liquid nitrogen, an URS-2.0 X-ray apparatus and the experimental system.

The test samples were lithium iodate α-$LiIO_3$ crystals (hexagonal system, point group C_6) grown by open evaporation in H_2O and natural muscovite mica $KAl_2[AlSi_3O_{10}](OH)_2$ plate-like crystals (monoclinic system, point group 2/*m*, prismatic) that are used for the production of electrically insulating materials, e.g., micanite and micafolium. These crystals were chosen as test samples because of their hydrogen bonds. For the tests we cut out, ground and polished several samples of each crystal, with a 0.05 mm thickness for plate-like muscovite crystals and 0.5–1 mm for lithium iodate.

The experimental system was developed, fabricated, patented [9] and used in this work under RBRF Grant No. 18-32-00656. The measurements were carried out in the 77–473 K range and at electric field frequencies of $1–10^8$ Hz. The design of the stationary device contains the following basic components (Fig. 3). A vacuum screening cap *3* made of stainless steel is mounted on a steel base plate *1*. A hollowed bottom electrode *4* is attached to the base plate with pipes *6* and *7* that are welded to a cap *5* and used for the supply and discharge of liquid nitrogen vapors and are attached to the base plate with fluoroplastic washers *24* and retaining nuts *25*. The bottom surface

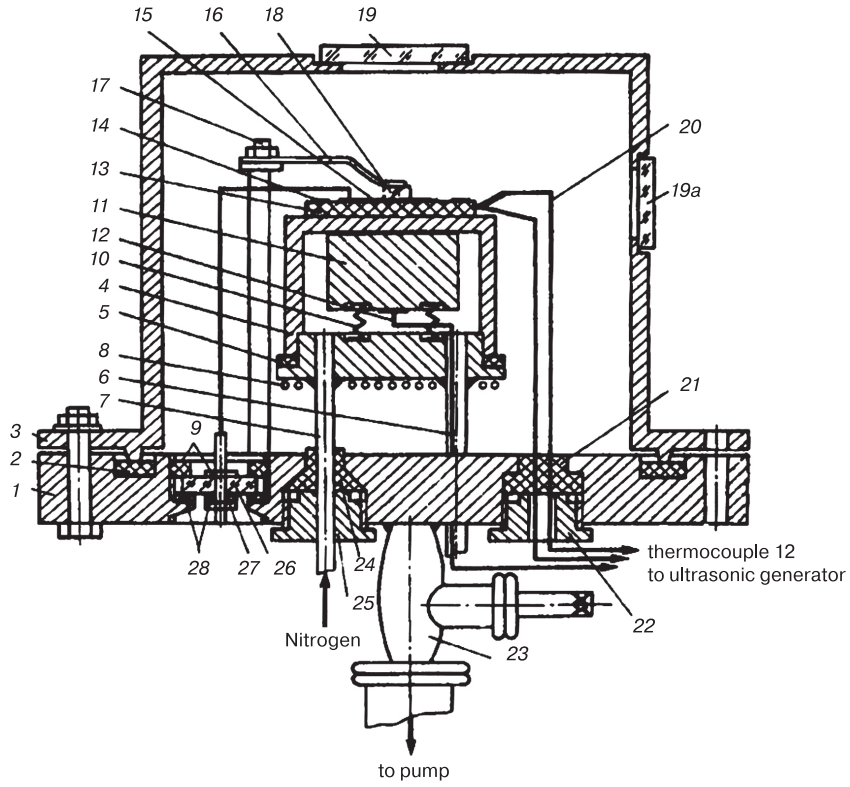

Figure 3. Multifunctional system for studying physical and technical parameters of semiconductors, dielectrics and electrically insulating materials.

of the cap of the bottom electrode *4* has a direct current powered heater coil *8* contained in quartz pipes.

An ultrasonic converter *11* having an output *12* to an ultrasonic generator is attached with springs *10* inside the electrode *4*. The test sample *13* with a guard electrode *14* and a measuring electrode *15* is placed onto the hollowed bottom electrode *4* and slightly pressed down with a thin spring plate *16* attached to an isolated pole *17* and a molten quartz plate *18*. The vacuum electric input consists of a molten quartz plate *26* with a centered hole for the input of a contact *27*. The natural sample heating rate was preferably 0.5–1.0 K/min. The pressure inside the system was maintained at 10^{-3}–10^{-4} mm Hg with a roughing vacuum pump and a diffusion pump through a union *23*. The vacuum screening cap has windows *19* and *19a* for sample irradiation and reflected radiation detection with a photoelectron amplifier. The temperature is measured with two differential Chromel-Copel thermocouples *20* at the bottom and top electrodes through a contact *21* with a retaining nut *22*. The vacuum electric input is assembled from the molten quartz plate *26* with a centered hole for the input of the contact *27*. The measurement error of this system is as follows: $\pm 1 \times 10^{-15}$ A for current, 5% for tgδ at $\text{tg}\delta \geq 5 \times 10^{-4}$, 10–30% for tgδ at $1 \times 10^{-4} \leq \text{tg}\delta < 5$ and 2% for electrical capacity.

5. Results and discussion

The object of this study is achieved by comparing the TSD spectra of the crystals taken along the optical axis with the TSD spectra taken perpendicular to the optical axis and with the TSL and electrical conductivity spectra. The fundamentals of this technology were put forward by us earlier [10] and partially described [11].

We now consider the suggested diagnostic method for the example of hexagonal lithium iodate crystals α-$LiIO_3$ used in laser engineering. The method is implemented as follows. The sample of the test material is silver coated at two sides by vacuum sputtering in a VUP-5 plant for producing silver electrodes. Alternatively contactode or glue electrodes made from AK-113 lacquer and fine nickel powder can be used to provide for similar results. The sample is thermostated at T_p = 300 K accurate to ±0.5 K. If the material contains polar defects they will be detected as maxima in the TSD spectrum on a recorder or on a computer display. Then the resultant spectra taken along and perpendicular to the sixth order optical axis of the crystal are examined, and their comparison reveals the presence of anisotropy and the direction of the optical axes. The measurements were carried out for different samples cut from one crystal in order to eliminate the effect or residual polarization.

Of the 32 known classes of crystalline dielectrics, pyroelectrics are 10 classes which are non-centrosymmetric and have a polar axis. This group also includes hexagonal crystalline lattice crystals to which lithium iodate crystals pertain. Anisotropy is the dependence of physical properties (in the case considered, electrical and optical ones) on direction in the crystal.

If a crystal is pyroelectric this should be seen from its TSD spectrum. We will now dwell upon this phenomenon.

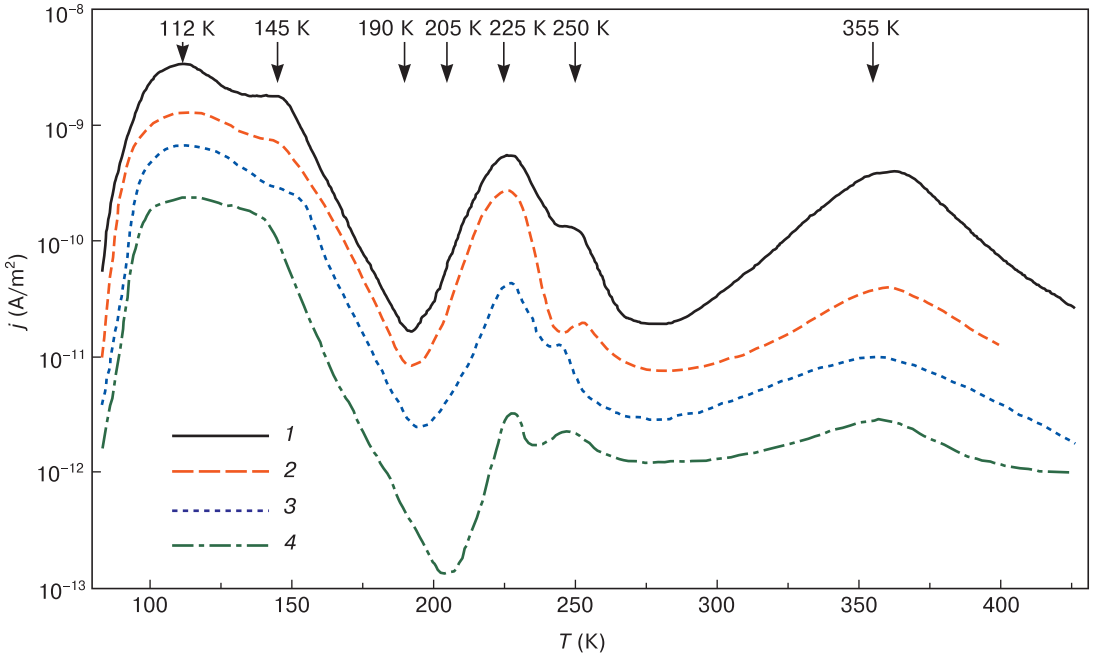

Figure 4. TSD current density of α-$LiIO_3$ single crystals along [0001] axis as a function of E_p for T_p = 323 K, t_p = 10 min, d = 0.7 mm, electrode diameter 25 mm and E_p field magnitudes, V/m: (*1*) 8.5×10⁵; (*2*) 4×10⁵; (*3*) 2×10⁵; (*4*) 5×10⁴.

The pyroelectric effect is caused by the appearance and accumulation of electric charge on crystal surface during crystal heating or cooling, resulting in the production of an electric moment [12] due to a change in the spontaneous polarization during temperature variation. Pyroelectric currents are produced due to variations in the temperature of a pyroelectric material (Fig. 4).

Heating of electrets also produces currents which are however accounted for by depolarization. For these crystals the magnitude of these currents decreases with time, with the pattern of the TSD spectrum changing significantly. Indeed the experiment showed that the first and second TSD spectrum maxima of lithium iodate at 112 and 145 K are reproduced from experiment to experiment. It is noteworthy that the method of partial thermal cleaning does not hold for the TSD current maxima Nos. 1 and 2 at 112 and 145 K: these maxima are not suppressed after reheating from the liquid nitrogen temperature. The method of partial thermal cleaning however holds well for higher temperature maxima. Thus pyroelectric current (maxima 1 and 2) dominates over weak relaxation current by 3–4 orders of magnitude. The activation energies (Table 1) calculated from the TSD spectra agree well with the activation energies calculated from infrared spectra [13, 14].

Table 1. Activation energy and concentration of relaxers for α-$LiIO_3$ crystals

Maximum No.	T_m, K	$U_a \parallel Z$ axis, eV	Concentration $\parallel Z$ axis, m^{-3}	$U_a \perp Z$ axis, eV	Concentration $\perp Z$ axis, m^{-3}
1	112	0.07 ± 0.02	–	–	–
2	145	0.15 ± 0.02	1.2×10^{18}	0.16 ± 0.03	3.8×10^{8}
3	190	0.30 ± 0.03	–	–	–
4	205	0.35 ± 0.03	–	–	–
5	225	0.42 ± 0.04	–	–	–
6	250	0.48 ± 0.05	5.4×10^{20}	0.50 ± 0.05	2.4×10^{15}
7	352	0.45 ± 0.05	8×10^{22}	0.65 ± 0.06	4.7×10^{17}

It was shown [12] that the pyroelectric coefficient of lithium iodate has a broad maximum at 120–140 K (Fig. 5). It can also be seen from Fig. 5 that the pyroelectric coefficient of lithium iodate is also large at 100 K, confirming the presence of pyroelectric current in the Z direction of the test crystal (sixth order axis [0001]).

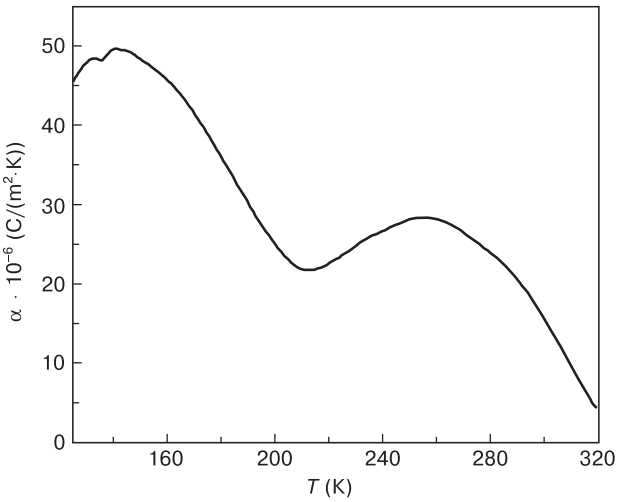

Figure 5. Temperature dependence of pyroelectric effect in α-$LiIO_3$ single crystals [12].

Study of the TSD spectra that were also described earlier [15] showed that the temperatures of the maxima in the TSD spectra (Fig. 4) and the TSL spectra (Fig. 6) [6] coincide and hence there is a direct relationship between the thermally activated and relaxation phenomena. The samples were X-ray irradiated on an URS-2.0 apparatus with a BSV-2 tube (Cu, 12 kV, 10 mA). The TSL spectra were recorded with a FEU-92 photoelectron amplifier and a DC amplifier and visualized with

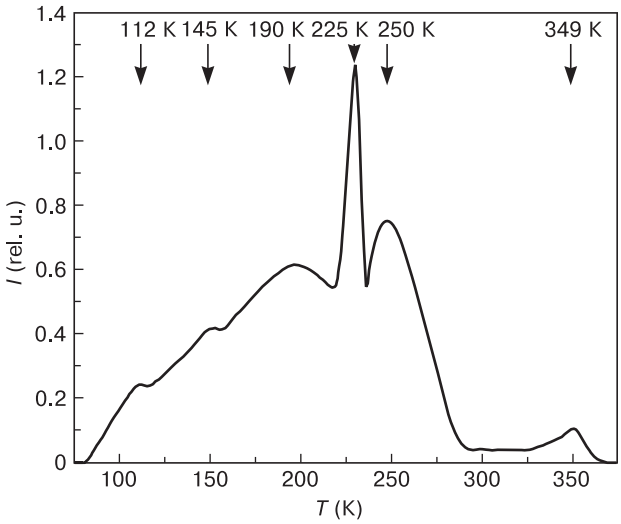

Figure 6. Thermally stimulated luminescence spectrum of α-$LiIO_3$ crystals: t_p = 1 h, U = 15 kV, T_p = 80 K. Irradiation on URS-2.0 X-ray apparatus. t_p, U and T_p are polarization time, voltage and temperature, respectively.

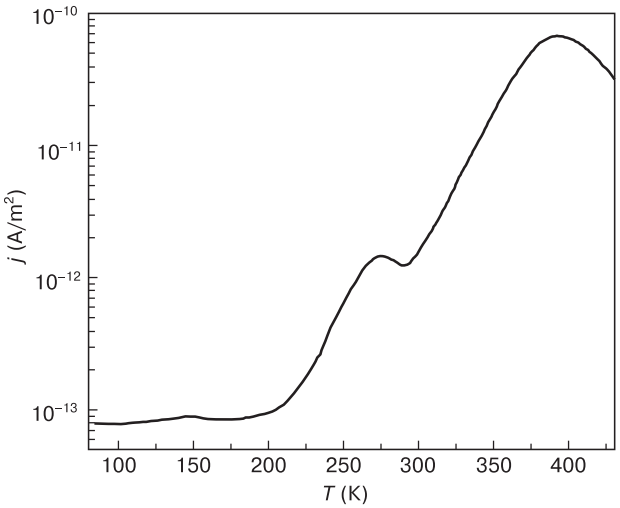

Figure 7. TSD spectrum of α-$LiIO_3$ crystals taken perpendicular to the sixth order axis at $E_p = 4 \times 10^5$ V/m and T_p = 376 K.

a KSP-14 recorder. FEU-92 was powered from a stabilized high-voltage power source.

Most crystalline materials having defect-free lattices exhibit small if any photoluminescence.

However an impurity ion concentration of a few hundredths of a percent is sufficient to initiate luminescent properties in these materials. Recombination luminescence is excited in solid crystalline materials as a result of the generation of metastable carriers (electrons or holes) due to the action of an ionizing radiation source. This is the so-called defect or impurity center luminescence. Any luminescence process can include carrier trapping by traps or mobile defects followed by carrier release upon heating.

As can be seen from the experimental results (Fig. 6) luminescence involves the defects which show themselves in the TSD spectra (Fig. 4). Under exposure to X-rays an electron moves across the crystal until recombination with an ionic defect or trapping. Luminescence is produced in the former case. In the latter case part of electrons end up localized at trapping centers (in the crystals considered these are H_3O^+, impurity water molecules). Obviously an electron can only be trapped by a mobile defect, i.e., if it is "defrosted" which is the case when maxima appear in the TSD spectra. In the case considered these defects are H^+, OH^-, H_3O^+ and water molecules. The probability of hydrogen ions in lithium iodate crystals was first predicted in earlier works [16, 17].

Comparison of Figs 4 and 7 shows that that the TSD spectra taken along the optical axis of lithium iodate crystals contain 7 maxima including the pyroelectric current ones (maxima Nos. 1 and 2, Fig. 4) while the TSD spectra taken perpendicular to the optical axis contain only 3 weak maxima and none of which corresponds to pyroelectric current (Fig. 7). The relaxer concentrations along and perpendicular to the sixth order axis for the three TSD maxima being compared differ significantly (Table 1) which suggests the directions of the crystallographic axes and confirms the presence of anisotropy in this crystal.

Thus study of thermally stimulated depolarization current spectra allows diagnostics [21] of anisotropy of optical axes in crystals and pyroelectric currents which in turn also confirm the presence of anisotropy. This means that the technology suggested herein is suitable both for pyroelectrics and non-pyroelectric crystals.

For muscovite mica crystals (Fig. 8) the TSD spectra taken along the direction perpendicular to the (001) face contain 7 TSD maxima having similar behavior in response to variation of different parameters and impurities. Taking TSD spectra for other directions in muscovite mica crystals is impossible because the thickness of a mica plate is only 5 mm. Since muscovite does not pertain to polar symmetry classes it does not exhibit pyroelectric properties. However the presence of TSD spectra similar to those of lithium iodate confirms the presence of anisotropy. Similar conclusions can be drawn for phlogopite and a number of other crystals.

The conclusions made on the basis of the experimental TSD spectra are confirmed by analysis of the IR spectra [14] and electrical conductivity (Fig. 9).

It can be seen from Fig. 9 that the electrical conductivity in the direction along the optical axis (Curve *1*) is almost three orders of magnitude higher than that in the direction perpendicular to the optical axis (Curve *6*), and this is confirmed by earlier data [19–21]. Study of anisotropy in optical crystals with a protonic conductivity type e.g. lithium iodate [22, 23] with the use of strong light beams is inexpedient since the contact of radiation with the crystal surface leads to accumulation of stress and cracking along cleavage planes or along block boundaries. This reduces the beam resistance of the crystals, increases the dislocation density and light absorption in the crystals and eventually leads to beam scattering and laser power degradation. Electrical measurements do not cause these detrimental consequences.

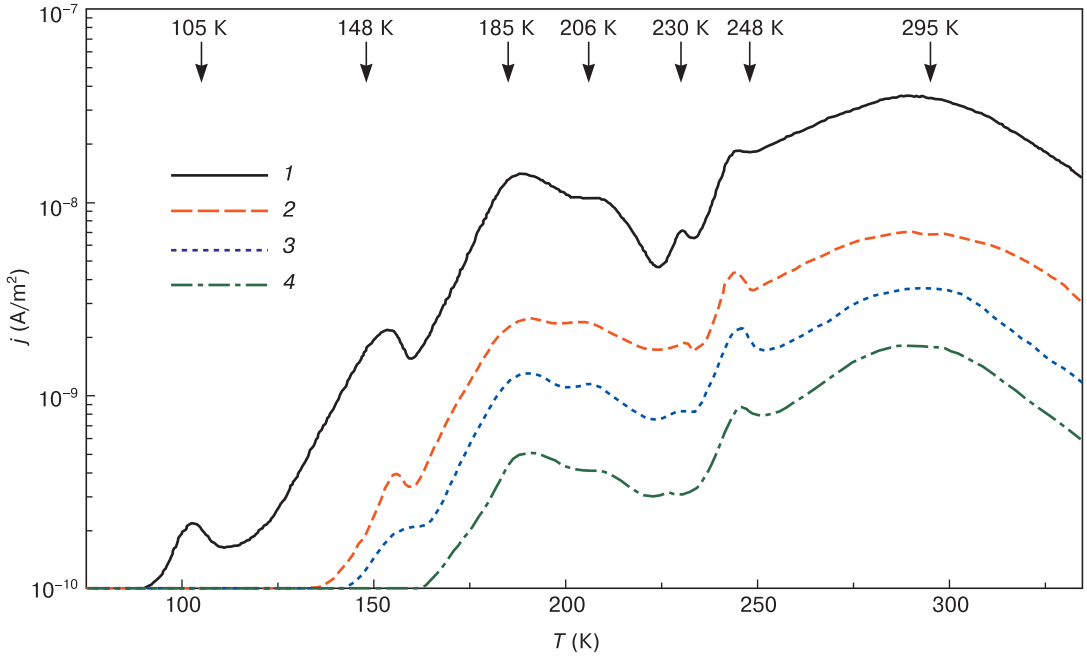

Figure 8. Muscovite mica TSD current density as a function of E_p for T_p = 323 K and t_p = 10 min for E_p field magnitudes, V/m: (*1*) 5×10^6; (*2*) 10^6; (*3*) 5×10^5, (*4*) 2×10^5.

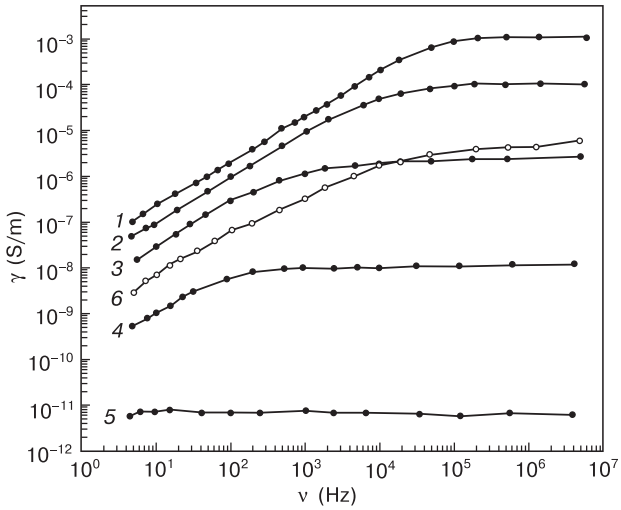

Figure 9. Frequency dependence of electrical conductivity of α-$LiIO_3$ crystals at temperatures of (*1*) 297, (*2*) 265, (*3*) 229, (*4*) 183 and (*5*) 125 K along the optical axis and (*6*) 297 K perpendicular to the optical axis.

6. Conclusion

The reported TSD examination experiments for muscovite and lithium iodate crystals suggest that the technology suggested in this work allows not only detecting the presence of anisotropy and determining optical axis directions but also evaluating the quality of optical crystalline materials. In spite of the different principles underlying the TSL and TSD studies, the experiment showed exact coincidence of the temperatures of maxima in the TSL and TSD spectra indicating that the same defects participate in both processes. The data obtained using the TSD method for determining the direction of the optical axis in crystals agree well with the temperature and frequency spectra of electrical conductivity. Furthermore the TSD method not only detects the presence of anisotropy but also gives the exact direction of the optical *Z* axis [0001] along which the spectrum contains seven maxima whereas the spectrum taken perpendicular to the optical axis contains only three maxima.

The use of the thermally stimulated depolarization current method allowed completely solving the tasks of this work and puts forward a technology for the diagnostics of anisotropy and optical axes in crystalline materials. The technology developed in this work is doubtlessly of interest for the fundamental research dealing with the tunneling effect and for various practical applications as a method of examining the quality of optical crystals at a sufficiently high scientific and technical level that was unachievable before, resulting in the consequent development of the method of optical diagnostics of optical axes and types of oscillation centers in crystals with hydrogen bonds [13, 14].

Low-temperature studies are important for applications in extreme north and Antarctic regions where temperatures below –50 °C occur at which the electrophysical and optical parameters of crystalline materials change.

Acknowledgements

The work was carried out with support from RBRF Grant No. 18-32-00656 mol_a (Study of relationship between optical-luminescent and mechanical phenomena due to reversible ionization of Ce^{3+} activator in Lu_2SiO_5:Ce^{3+} single crystals).

References

1. Pat. 2442972 (RF). *Sposob opredeleniya polozheniya opticheskoi osi fazovoi anizotropnoi kristallicheskoi plastinki λ/4* [Method for determining the position of the optical axis of the phase anisotropic crystal plate λ/4]. O.Yu. Pikul, 2012. (In Russ.)
2. Certificate of authorship 737822 (USSR). *Sposob opredeleniya vida defektov, ikh kolichestva, energii aktivatsii, vremeni relaksatsii, aktivatsionnykh obemov defektov kristallicheskoi reshetki dielektrikov i poluprovodnikov i ustroistvo dlya ego realizatsii* [Method for determining the type of defects, their number, activation energy, relaxation time, activation volumes of crystal lattice defects in dielectrics and semiconductors and a device for its implementation]. V.I. Bulakh, V.A. Mironov, M.P. Tonkonogov, 1980. (In Russ.)
3. Pat. 2347216 (RF). *Sposob opredeleniya temperatury poyavleniya tunnel'nogo effekta v dielektrikakh i elektroizolyatsionnykh materialakh* [Method for determining the temperature of the tunnel effect in dielectrics and electrical insulation materials]. V.M. Timokhin, 2009. (In Russ.)
4. Bucci C. Ionic thermocurrents in alkali halide crystals containing substitutional beryllium ions. *Phys. Rev.*, 1967; 164(3): 1200. https://doi.org/10.1103/PhysRev.164.1200
5. Bucci C., Fieschi R. Ionic thermoconductivity. Method for the investigation of polarization in insulators. *Phys. Rev. Lett.*, 1964; 12(1): 16–19. https://doi.org/10.1103/PhysRevLett.12.16
6. Johary G.P., Jones S.J. Study of the low-temperature "transition" in ice I_h by thermally stimulated depolarization measurements. *J. Chem. Phys.*, 1975; 62(10): 4213–4223. https://doi.org/10.1063/1.430303
7. Takei I., Maeno N. Dielectric properties of single crystals of HC1-doped ice. *J. Chem. Phys.*, 1984; 81(12): 6186–6190. https://doi.org/10.1063/1.447573
8. Gorokhovatsky Yu.A. *Osnovy termodepolyarizatsionnogo analiza* [Fundamentals of thermodepolarization analysis]. Moscow: Nauka,1981: 173. (In Russ.)
9. Pat. 2348045 (RF). *Mnogofunktsional'noe ustroistvo dlya issledovaniya fiziko-tekhnicheskikh kharakteristik poluprovodnikov, dielektrikov i elektroizolyatsionnykh materialov* [Multifunctional device for research of physical and technical characteristics of semiconductors, dielectrics and electrical insulating materials]. V.M. Timokhin, 2009. (In Russ.)
10. Timokhin V.M. Tunnel effect in widezone crystals with proton conductivity. *J. Nano and Electronic Phys.*, 2014; 6(3): 03048 (3pp).
11. Timokhin V.M. *Fizika dielektrikov. Termoaktivatsionnaya i dielektricheskaya spektroskopiya kristallicheskikh materialov. Protonnyi transport* [Physics of dielectrics. Thermal activation and dielectric spectroscopy of crystalline materials. Proton transport]. Moscow: Izdatel'skiy dom MISiS, 2013: 258. (In Russ.)
12. Bhalla A.S. Low temperature puroelectric properties of α-$LiIO_3$ single crystals. *J. Appl. Phys.*, 1984; 55(4): 1229–1230. https://doi.org/10.1063/1.333170
13. Timokhin V.M., Garmash V.M., Tedzhetov V.A. Spectral diagnostics of vibrational centers in crystals with hydrogen bonds. *Izvestiya Vysshikh Uchebnykh Zavedenii. Materialy Elektronnoi Tekhniki = Materials of Electronics Engineering*, 2019; 22(1): 35–44. (In Russ.). https://doi.org/10.17073/1609-3577-2019-1-35-44
14. Timokhin V.M. Garmash V.M., Tedzhetov V.A. Infrared spectroscopy and tunneling of protons in crystals with hydrogen bonds. *Optics and Spectroscopy*, 2017; 122(6): 889–895. https://doi.org/10.1134/S0030400X17060224
15. Tedzhetov V.A., Podkopaev A.V., Sysoev A.A. Study of the energy band structure of Lu_2SiO_5 : Ce^{3+} single crystals by thermally stimulated luminescence method. *IOP Conf. Ser.: Mater. Sci. Eng.*, 2019; 525: 012044. https://doi.org/10.1088/1757-899X/525/1/012044
16. Blistanov A.A. *Kristally kvantovoi i nelineinoi optiki* [Crystals for quantum and nonlinear optics]. Moscow: MISiS, 2000: 432. (In Russ.)
17. Fillaux Fr. Proton transfer in the $KHCO_3$ and acid crystals: a quantum view. *J. Molecular Structure,* 2007; 844–845: 308–318. https://doi.org/10.1016/j.molstruc.2007.05.046
18. Plyusnina I.I. *Infrakrasnye spektry silikatov* [Infrared spectra of silicates]. Moscow: MGU, 1967: 190. (In Russ.)
19. Yaroslavtsev A.B. Proton conductivity of inorganic hydrates. *Russ. Chem. Rev.*, 1994; 63(5): 429–435. https://doi.org/10.1070/RC1994v063n05ABEH000095
20. Ivanov Yu.N., Sukhovsky A.A., Aleksandrova I.P., Totz J., Michel D. The mechanism of proton conductivity in the crystals of NH_4SeO_4. *Fizika tverdogo tela*, 2002; 44(6): 1032–1038. (In Russ.)
21. Timokhin V.M. The mechanism of dielectric relaxation and proton conductivity in α-$LiIO_3$ nanostructure. *Russ. Phys. J.*, 2009; 52(3): 269–274. https://doi.org/10.1007/s11182-009-9221-8
22. Pat. 2566389 (RF). *Termostimulirovannyi sposob diagnostiki anizotropii opticheskikh osei kristallov* [Thermally stimulated current method of diagnosis of the anisotropy of the optical axes of the crystals]. V.M. Timokhin, 2015. (In Russ.)
23. Timokhin V.M., Garmash V.M., Tarasov V.P. NMR spectra and translational diffusion of protons in crystals with hydrogen bonds. *Phys. Solid State*, 2015; 57(7): 1314–1317. https://doi.org/10.1134/S1063783415070331